Article

Cell

# A Reservoir of Mature Cavity Macrophages that Can Rapidly Invade Visceral Organs to Affect Tissue Repair

## Graphical Abstract

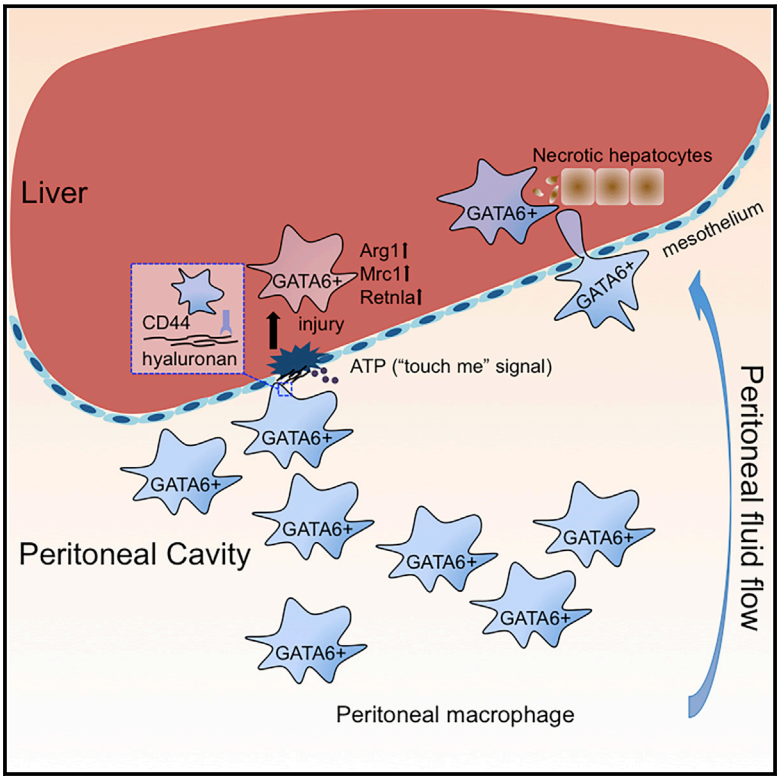


## Highlights

- Peritoneal macrophages rapidly infiltrate an injured visceral organ
- Infiltration occurs via a non-vascular route and can go into deeper tissue
- Peritoneal macrophages in injury site adopt an alternatively activated phenotype
- Depletion of peritoneal macrophages results in lethality in acute liver injury

## Authors

Jing Wang, Paul Kubes

## Correspondence

pkubes@ucalgary.ca

## In Brief

Following a sterile injury to visceral organs like the liver, a reservoir of fully mature peritoneal cavity macrophages infiltrates the afflicted tissue within an hour via a non-vascular route, isolating the injury and contributing to tissue repair.

Wang & Kubes, 2016, Cell *165*, 668–678
April 21, 2016 
http://dx.doi.org/10.1016/j.cell.2016.03.009

CellPress

Cell

Article

# A Reservoir of Mature Cavity Macrophages that Can Rapidly Invade Visceral Organs to Affect Tissue Repair

Jing Wang[1,2] and Paul Kubes[1,2,*]
[1]Department of Physiology and Pharmacology
[2]Immunology Research Group
Snyder Institute for Chronic Diseases, Cumming School of Medicine, University of Calgary, Calgary, AB T2N 4N1, Canada
*Correspondence: pkubes@ucalgary.ca
http://dx.doi.org/10.1016/j.cell.2016.03.009

## SUMMARY

A key feature of inflammation is the timely recruitment of leukocytes, including monocytes, from blood into tissues, the latter maturing into macrophages over a period of 2–3 days. Using multi-channel spinning disk microscopy, we identified a rapid pathway of macrophage recruitment into an injured organ via a non-vascular route requiring no maturation from monocytes. In response to a sterile injury in liver, a reservoir of fully mature F4/80$^{hi}$GATA6$^{+}$ peritoneal cavity macrophages rapidly invaded into afflicted tissue via direct recruitment across the mesothelium. The invasion was dependent on CD44 and DAMP molecule ATP and resulted in rapid replication and switching of macrophage toward an alternatively activated phenotype. These macrophages dismantled the nuclei of necrotic cells releasing DNA and forming a cover across the injury site. Rapid invasion of mature macrophages from body cavity with capacity for induction of reparative phenotype may impact altered tissues ranging from trauma to infections to cancer.

## INTRODUCTION

Inflammation in response to infection or sterile injury has been studied extensively, and certain fundamental principles have been well established. During inflammation, resident tissue macrophages as well as mast cells and other parenchymal cells are activated, stimulating endothelium to express adhesion molecules that then induce the recruitment of multiple cell types (Kim and Luster, 2015). In most cases, neutrophils are the first cells to arrive at the afflicted tissue potentially killing pathogens or clearing debris before they undergo apoptosis. A robust recruitment of monocytes ensues, and these cells are thought to remove dying neutrophils and eventually differentiate into macrophages or dendritic cells over a few days and promote tissue remodeling (Serhan et al., 2007). The tissue resident macrophages are thought to coordinate many of these events, and in some cases these cells can increase their numbers at the source through self-replication (Davies et al., 2013b; Jenkins et al., 2011). The monocyte recruitment and differentiation, however, becomes more essential if tissue is severely damaged eradicating the tissue resident macrophages. For example, *Listeria monocytogenes* infection induces early necroptotic death of the liver resident macrophages, the Kupffer cells. This triggers the proliferation and alternative activation of the recruited monocyte-derived macrophages and ultimately replaces the dead Kupffer cells (Blériot et al., 2015). In sterile inflammation, it has been shown that resident macrophages are lost after adult cardiac injury and are instead replaced by inflammatory monocyte-derived macrophages (Lavine et al., 2014). Since there is no circulating population of macrophages, a rapid recruitment of these cells is thought not to be possible.

Most vertebrates have a number of defined body cavities, surrounding the internal organs including the peritoneal cavity in which the visceral organs reside, the pleural cavity in which the lung is found and the pericardial cavity where the heart is situated. Macrophages in the peritoneal cavity have been studied extensively for their ability to phagocytose and kill invading pathogens. Recently, two physically, functionally, and developmentally different peritoneal macrophage subsets have been described (Ghosn et al., 2010). The small peritoneal macrophages (SPMs) are F4/80 low, CD11b low, and Ly6C positive, and bone marrow derived and are present as a small population under basal conditions but can be recruited from a pool of circulating monocytes into the peritoneum upon infection. SPMs phagocytose bacteria and make large amounts of nitric oxide. By contrast the large peritoneal macrophages (LPMs) are F4/80 high, CD11b high, and Ly6C negative. LPMs are maintained in the peritoneal cavity through self-renewal and are capable of undergoing rapid proliferation upon inflammation (Jenkins et al., 2011). Compared to SPMs, LPMs make much less nitric oxide and have less capacity to phagocytose bacteria. However, LPMs phagocytose apoptotic cells more effectively (Uderhardt et al., 2012). Recently, further characterization of the peritoneal macrophages revealed that LPMs but not SPMs selectively express the zinc finger transcription factor GATA-binding protein 6 (GATA6) (Gautier et al., 2014; Okabe and Medzhitov, 2014; Rosas et al., 2014). Gata6-deficient mice have fewer LPMs, and Gata6 appears to be involved in

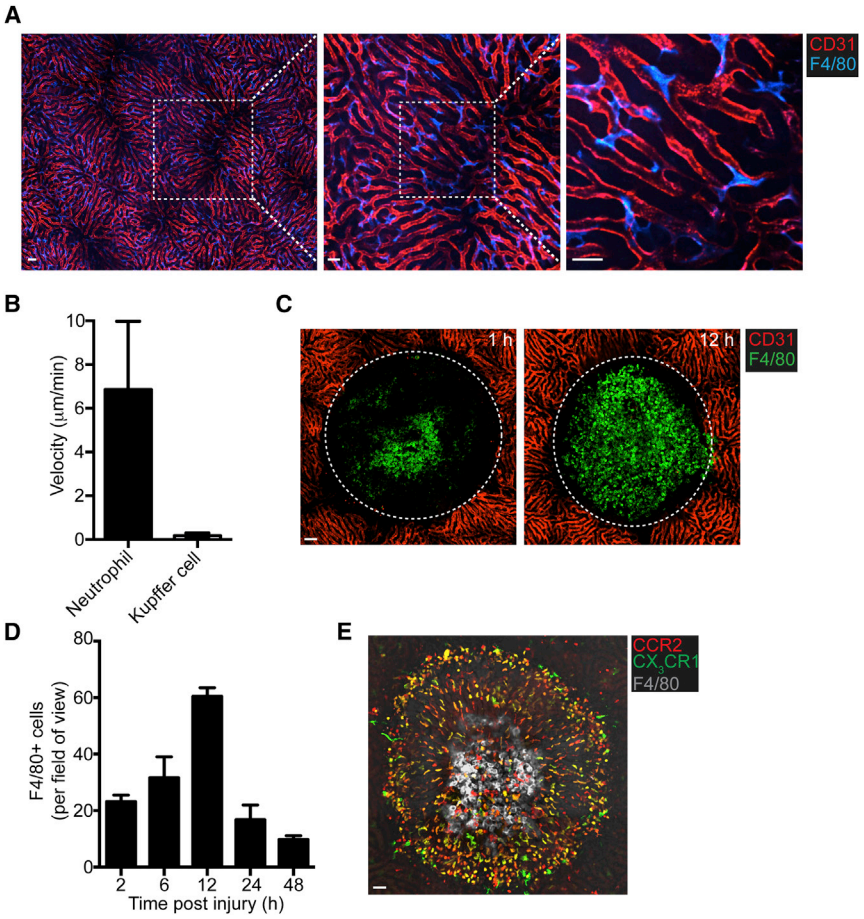


**Figure 1. Rapid Accumulation of F4/80$^{hi}$ Macrophages in Sterile Injury in Liver**

(A) Distribution of F4/80$^{hi}$ macrophages (blue) in liver sinusoid (red) at basal condition. Higher magnification of the indicated area (box) was shown in middle and right. Scale bars, 50 (left) and 20 (middle and right) μm.

(B) Crawling velocities of neutrophils and Kupffer cells responding to tissue injury. Experiments were conducted 2 hr post-injury. Error bars represent SEM, n = 3.

(C) Visualization of F4/80$^{hi}$ population (green) in injury by topically applying F4/80 antibody. Mice were intravenously injected with anti-CD31 (red) to visualize liver vasculature. Injury border was delineated with a white dashed line. Images are representative of at least ten experiments. Scale bars, 20 μm.

(D) Quantification of F4/80$^{hi}$ cells that accumulated within injury at indicated time points. Error bars represent SEM n = 3 for each time point.

(E) Representative intravital image of F4/80$^{hi}$ cells (gray) in *Ccr2*$^{RFP/+}$/*Cx3cr1*$^{GFP/+}$ mouse (CCR2: red; $CX_3CR1$: green) at 24 hr post-focal injury. Images are representative of five experiments.

Scale bars, 15 μm. See also Movies S1, S2, and S3.

the control of the proliferation, survival, and metabolism of these cells.

In this study, we have documented that these cavity macrophages defy many of the aforementioned principles regarding immobilized tissue resident macrophages including their ambulatory non-fixed nature. Using a simple sterile thermal injury model of the liver, we have identified that GATA6$^{+}$ macrophages infiltrate within 1 hr directly into the liver injury site from the peritoneum in response to ATP released by necrotic cells. Rather than using the traditional intravascular integrin recruitment pathways, these macrophages use CD44 to bind to exposed hyaluronan at the injury site. These fully mature macrophages rapidly proliferate and adopt an alternative activation phenotype once they are located in the afflicted tissue. Intravital imaging revealed that these cells dismantle nuclei from necrotic cells and help to fully revascularize the site of injury. Last, using a more complex liver fibrosis model, we found that peritoneal macrophages relocate from peritoneum into the liver parenchyma by migrating across the mesothelial layer that covers the liver and invade deep into the tissue. Depletion of peritoneal macrophages results in lethality in an acute liver injury model. Our data describe a non-vascular recruitment, of a reservoir pool of body cavity macrophages into visceral organs and demonstrate their essential functions for tissue repair.

## RESULTS

### Rapid Accumulation of Macrophages following Sterile Injury in Liver

Administration of F4/80 antibody into the blood stream labeled liver macrophage, namely, Kupffer cells. These cells resided in the blood vessels of the liver, and exclusively in sinusoids (Figure 1A). Kupffer cells were completely immobile and constantly probing the local environment with their multiple pseudopods. No motile F4/80-positive cells were noted in the liver vasculature (Movie S1). Touching a heated thermo probe to the surface of the liver caused all cells inside an area of approximately 600 μm in diameter to be killed and intravital imaging over long periods showed no F4/80$^{hi}$ cells moving intravascularly into the injury site (Dal-Secco et al., 2015; McDonald et al., 2010) (Figure 1B; Movie S2). However, administration of F4/80 antibody topically to the injury site revealed an F4/80$^{hi}$ population of cells accumulating as early as 1 hr post-injury. The accumulation of these cells peaked at 12 hr and persisted for at least 48 hr (Figures 1C and 1D). Our previous study has shown that CCR2$^{high}$ inflammatory monocytes entered the site starting at 8 hr and $CX_3CR1^{high}$ monocytes appeared around the injury site at 24–48 hr. Flow cytometry analysis suggested neither of these monocyte populations expressed F4/80, Mertk, or other macrophage markers in the first 72 hr (Dal-Secco et al., 2015). To further confirm the early accumulation of F4/80$^{hi}$ cells were not derived from monocytes, F4/80 antibody was applied to the lesion in *Ccr2*$^{RFP/+}$/*Cx3cr1*$^{GFP/+}$ reporter mouse, which showed an abundance of monocyte recruitment at 24 hr post-injury. These monocytes were highly heterogeneous, expressing different levels of CCR2 and

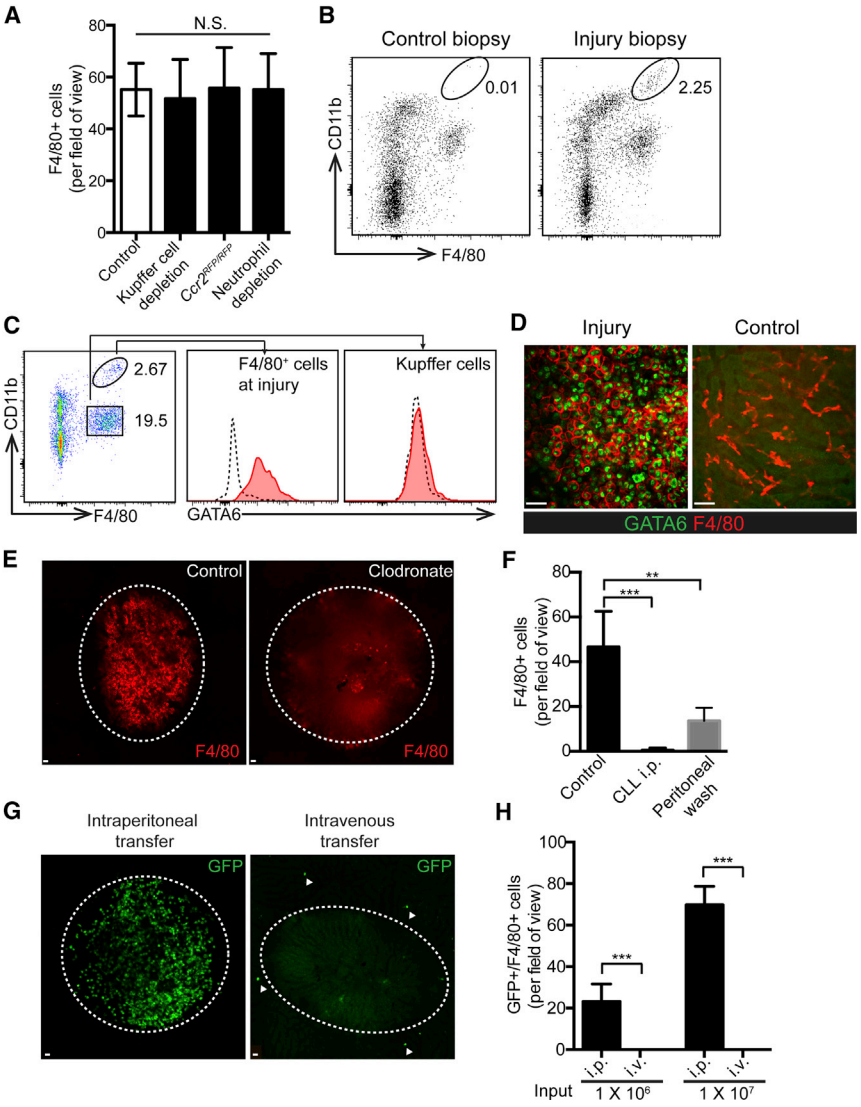


**Figure 2. GATA6$^{+}$ Peritoneal Macrophages Are Accumulating at Sterile Injury**

(A) Quantification of F4/80$^{hi}$ cells within the focal injury in wild-type mice that were previously treated with clodronate liposome (Kupffer cell depletion) or anti-Ly6G mAb (neutrophil depletion) or in *Ccr2*$^{RFP/RFP}$ mice. n = 3. Data were pooled from three independent experiments.

(B) Flow cytometry analysis for cells isolated from injury biopsy or control biopsy of uninjured tissue at 12 hr post-focal injury. Cells were pregated on size, viability, CD45$^{+}$, and Ly6G$^{-}$. Data are representative of three independent experiments.

(C) Flow cytometry analysis for GATA6 expression of macrophage subsets in injury biopsy harvested at 12 hr post-injury. Red, GATA6; dotted line, isotype control. Cells were pregated on size, viability, CD45$^{+}$, and Ly6G$^{-}$. Plots are representative of at least five independent experiments.

(D) Immunofluorescence staining for GATA6 (green) and F4/80 (red) of injury biopsy and control sections. Scale bars, 25 μm. Data are representative of two independent experiments.

(E) Representative images of F4/80$^{hi}$ cells within the 12-hr focal injury in mice that were previously treated with PBS liposome (control) or clodronate liposome (clodronate). The white dashed line highlights injury border. Scale bars, 20 μm.

(F) Quantification of F4/80$^{hi}$ cells within the focal injury in mice that were treated as indicated in (E) or having their peritoneal cavity rinsed by sterile saline. n = 5. Data were pooled from three independent experiments.

(G) Representative images of transferred LysM-eGFP peritoneal cells within the 12-hr focal injury in wild-type mice. 1 × 10$^{7}$ peritoneal cells isolated from LysM-eGFP mice were transferred through indicated route 1 hr prior to injury. The white dashed line highlights the injury border. Arrowheads indicate the GFP$^{+}$ cells in the liver sinusoid. Scale bars, 20 μm.

(H) Quantification of GFP$^{+}$ cells within the 12-hr focal injury in wild-type mice that received indicated numbers of peritoneal cells from LysM-eGFP mice.

Error bars represent SEM. **p < 0.01, ***p < 0.001, N.S., not significant. See also Figures S1 and S2.

CX$_3$CR1, yet none were co-localized with the F4/80$^{hi}$ cells (Figure 1E). Interestingly the F4/80$^{hi}$ cells appeared to be localized toward the center of the wound unlike the CCR2$^{high}$ monocytes that were recruited from the vasculature surrounding the wound and migrating inward (Figure 1E). Three-dimensional reconstruction of the injury site revealed that these macrophages were localized on top of the necrotic cells (Movie S3). This was not as a result of the antibody not being able to penetrate deeper because topical application of neutrophil antibodies labeled neutrophils deep in the injury site (data not shown).

## Peritoneal Macrophages Respond to Liver Injury through Direct Migration from Peritoneal Cavity

Intravenous administration of clodronate liposome depleted Kupffer cells prior to the injury but did not affect the accumulation of the F4/80$^{hi}$ macrophages inside the injury (Figure 2A). *Ccr2*$^{RFP/RFP}$ mice, which have very few monocytes recruited to the injury site, still had comparable numbers of F4/80$^{hi}$ macrophage in injury compared to wild-type mice, suggesting that neither Kupffer cells nor monocytes contribute to the macrophages in injury. Finally, neutrophils migrating to the injury site have to crawl across F4/80-positive Kupffer cells. To ensure that the neutrophils were not simply taking up membranes from macrophages, we depleted neutrophils and still noted many F4/80$^{hi}$ cells in the injury (Figure 2A). To characterize this F4/80$^{hi}$ population, cells were isolated from the injury biopsy; flow cytometry analysis suggested there was a distinct population expressing high levels of CD11b and F4/80 from injury biopsy samples compared to control biopsies taken from uninjured tissue (Figure 2B). We therefore examined expression of several macrophage related surface markers on this population and used Kupffer cells as an

internal reference. These cells were Ly6C$^{-}$, MHC-II$^{-}$, siglec-F$^{-}$, CD206$^{+}$, CD64$^{+}$, CD68$^{+}$, CD11c$^{+}$ CD115$^{low}$, and CD102$^{+}$, confirming they were macrophages but were different from Kupffer cells (Figure S1). Furthermore, CD102 has been identified as a specific marker for resident peritoneal macrophages and was present on macrophages in injury but not on Kupffer cells (Okabe and Medzhitov, 2014). Several recent studies have suggested that resident peritoneal macrophages selectively express a transcription factor, GATA6 (Gautier et al., 2014; Okabe and Medzhitov, 2014; Rosas et al., 2014) (Figure S2A). Indeed, these F4/80$^{hi}$ cells in the injury site were also positive for GATA6, revealed by both flow cytometry and immunofluorescent staining (Figures 2C and 2D). Expression of GATA6 was restricted to macrophages in the injury but not Kupffer cells (Figures 2C and 2D).

The above results suggested that peritoneal macrophages could be the source of the macrophages in injury. In fact, when peritoneal macrophages were depleted by intraperitoneal administration of clodronate liposome (CLL) (Figure S2B), no F4/80$^{hi}$ macrophages were found in the afflicted liver lesion (Figure 2E). However, Kupffer cells were still present in liver (as opposed to intravenous clodronate liposome administration). Washing out macrophages from peritoneal cavity also reduced F4/80$^{hi}$ macrophages in injury (Figures 2F and S2C). In addition, peritoneal cells from LysM-eGFP mice (Faust et al., 2000), in which >85% of the GFP$^{+}$ population are GATA6$^{+}$ macrophages, were adoptively transferred into the peritoneum of a non-GFP mouse (Figure S2D). As a result, abundant recruitment of GFP$^{+}$ cells were noted within the liver injury site (Figure 2G). Staining with F4/80 antibody confirmed the majority of GFP$^{+}$ cells were F4/80$^{hi}$ (Figure S2E). By contrast, LysM-eGFP peritoneal cells transferred into the vasculature failed to arrive at the liver injury (Figure 2G). Administration of a much larger amount of peritoneal cells intravenously induced some sticking of GFP$^{+}$ cells in the liver sinusoids, but no accumulation was noted in the injury site (Figures 2G and 2H). Long-term tracking of transferred GFP$^{+}$ cells also revealed that those cells were persistent in injury for about 72 hr and were completely gone at 120 hr (Figure S2F).

## Recruitment of Peritoneal Macrophages to Sterile Injury in Liver Is Dependent on ATP and CD44

To further investigate the mechanisms that guide peritoneal cavity macrophages into liver, mice were treated with pertussis toxin (PTX) to inhibit the Gαi-protein-coupled chemokine receptors (Lee et al., 2010). Macrophage accumulation was largely unaffected by PTX treatment (Figure 3A), suggesting macrophages in the peritoneal fluid were not attracted to the injury area by classical chemokine signaling. ATP released from dead cells can act as a damage-associated molecule-pattern (DAMP) (Kono and Rock, 2008). Mice pretreated with apyrase or ATP receptor antagonist demonstrated a significant reduction in the number of macrophages accumulated at injury (Figure 3B). Blocking β2-integrin (CD18), the dominant adhesion molecule used by circulating immune cells to reach sites of inflammation (Herter and Zarbock, 2013), had no effect on macrophage recruitment into the liver injury site (Figure 3C), suggesting that this recruitment of a reservoir of body cavity macrophages differs from intravascular recruitment of immune cells. β1-integrins are critical for adhesion to matrix proteins including collagen, fibronectin, and laminin. Blocking β1-integrins (CD29) did not reduce macrophage recruitment (Figure 3C). CD44 is an important adhesion molecule for recruitment of leukocytes to liver (Guidotti et al., 2015; McDonald et al., 2008; Shi et al., 2010). Pretreated mice with anti-CD44 antibody abolished the recruitment of macrophages (Figure 3D). In addition, preincubation of transferred LysM-eGFP$^{+}$ macrophages with anti-CD44 antibody demonstrated decreased macrophage recruitment to injury suggesting that the CD44 on macrophages is directly involved in mediating adhesion (Figure 3E). Indeed, CD44 is highly expressed on peritoneal macrophages (Figure S3). Hyaluronan, the ligand for CD44, has been shown to be removed effectively by hyaluronidase (McDonald et al., 2008). Pretreatment of the mice with this enzyme also prevented recruitment of macrophages to the injury site (Figure 3F). Immunofluorescent staining with hyaluronan binding protein revealed the exposed hyaluronan inside the injury area but not in the surrounding healthy tissue (Figure 3G).

## Alternative Activation of Peritoneal Macrophages upon Recruitment to Sterile Injury

Recent studies have revealed that hyaluronan can induce macrophages to switch their phenotype to alternatively activated macrophage (Rayahin et al., 2015). To determine whether the recruitment of the macrophages to the injured environment induced changes in their phenotype, we compared GATA6-positive macrophages from the peritoneum versus those from the injury biopsies. Only a small portion of resident peritoneal macrophages were positive for Ki67, a marker of proliferation, suggesting very little basal proliferation. In contrast, more than 20% of the macrophages from the biopsies expressed Ki67 at 12 hr post-injury (Figure 4A). Accordingly, bromodeoxyuridine (BrdU) pulse labeling showed that more than 10% of macrophages from the injury were in S phase at the early stage (Figure S4A). Local proliferation of resident macrophages is known as a signature for type 2 immune response (Jenkins et al., 2011). Indeed, the peritoneal macrophages were able to skew their phenotype toward alternative or repair macrophages, increasing their expression of CD273, CD206 (Figures 4B and 4D), and arginase 1 (Figures 4C and 4E), known as markers of alternatively activated macrophages (Huber et al., 2010; Martinez and Gordon, 2014). Measuring expression levels of these markers on macrophages over time revealed rapid elevation as early as 4 hr, which persisted for 48 hr (Figure 4F). qRT-PCR analysis also showed that the expression of alternative activation genes (*Chil3*, *Mrc1*, *Retnla*, *Il10*) was rapidly induced in the whole injury tissues from control mice but not peritoneal-macrophage-depleted mice (Figure S4B).

## Peritoneal Macrophages Disassemble Necrotic Cells and Contribute to Tissue Repair

Using intravital microscopy, we examined the behavior of peritoneal macrophages in the wound. The macrophages appeared to be constantly probing with a single pseudopod (Movie S4). To investigate how macrophages interact with necrotic cells, SYTOX Green was topically applied to the injury labeling the

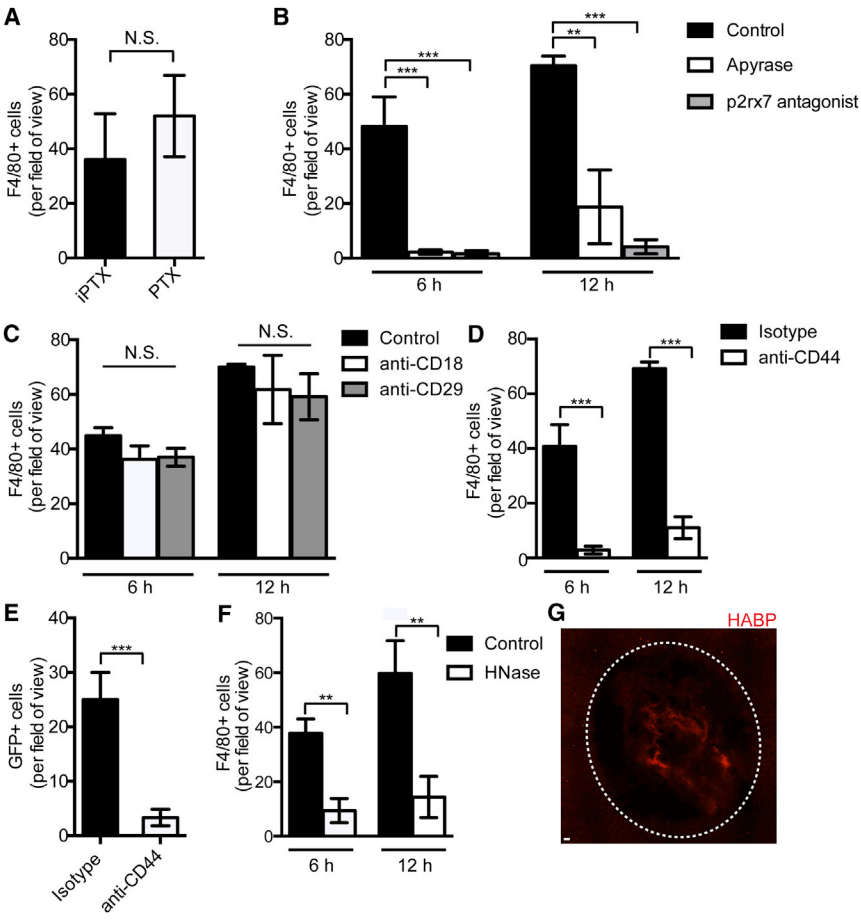


**Figure 3. Peritoneal Macrophages Are Attracted to Injury by Injury-Derived ATP and Hyaluronan**

(A) Quantification of F4/80$^{hi}$ macrophages within 12-hr focal injury in mice that were pretreated with inactivated pertussis toxin (iPTX) or pertussis toxin (PTX). n = 5. Data were pooled from three independent experiments.

(B) Quantification of F4/80$^{hi}$ macrophages within injury at indicated time points in mice that were pretreated with apyrase or p2rx7 antagonist. n = 5. Data were pooled from three independent experiments.

(C) Quantification of F4/80$^{+}$ macrophages within injury at indicated time points in mice that were pretreated with isotype control, anti-CD29, or anti-CD18 Abs. n = 3–5. Data were pooled from two independent experiments.

(D) Quantification of F4/80$^{hi}$ macrophages within injury at indicated time points in mice that were pretreated with isotype control or anti-CD44 Ab. n = 3–6. Data were pooled from three independent experiments.

(E) Quantification of GFP$^{+}$ cells in the 6-hr focal injury in wild-type mice that received peritoneal cells prior to injury. Peritoneal cavity cells harvested from LysM-eGFP mice were incubated with isotype control or anti-CD44 Abs and washed with PBS before adoptive transfer. n = 3. Data were pooled from three independent experiments.

(F) Quantification of F4/80$^{hi}$ macrophages within injury at indicated time points in mice that were pretreated with hyaluronidase. n = 3–5. Data were pooled from three independent experiments.

(G) Immunofluorescence staining of injury biopsy harvested 2 hr after injury induction with hyaluronic acid binding protein (HABP, red). The white dashed line highlights the injury border.

Scale bar, 10 μm. Error bars represent SEM. **p < 0.01, ***p < 0.001, N.S., not significant. See also Figure S3.

DNA in the nuclei of dead cells. Imaging over an extended period revealed microparticles of SYTOX Green being pulled from the nuclei by surrounding macrophages (Movie S5; Figure 5A). SYTOX Green staining revealed that the necrotic cells in a newly formed injury were intact and punctate nuclear structures (Figure 5B). The process of ripping pieces of nuclei released DNA and resulted in fewer intact nuclei. Instead, a layer of DNA covered the wound at 12 hr (Figure 5B). This could be eliminated by adding DNase I (Figures 5C and S5A). These were not neutrophil extracellular traps (NETs), as neutrophil depletion did not affect the formation of these structures (data not shown). Peritoneal macrophages were responsible for disassembling the necrotic nuclei as depletion of the peritoneal macrophages resulted in the SYTOX-Green-positive cells remaining intact nuclear structures and no DNA coverage was noted (Figure 5D). The injury was efficiently revascularized with newly restored sinusoids from the outer perimeter inward such that at 7 days the area of non-perfused tissue (assessed by CD31 antibody) was reduced by 75% (Figure 5E). In the absence of the influx of peritoneal macrophages, the healing was significantly delayed (Figures 5F and S5B).

## Decreased Peritoneal Macrophages in Sterile Injury and Delayed Tissue Repair in GATA6-Deficient Mice

Gata6 was described to be the key transcription factor for regulating survival and proliferation of the peritoneal macrophages and Gata6 deficiency affected multiple transcriptional networks (Gautier et al., 2014; Rosas et al., 2014). We therefore used Lyz2-Cre × Gata6$^{flox/flox}$ mice (Mac-*Gata6* knockout [KO]) to address whether Gata6 deficiency will affect the response of peritoneal macrophages to injury. Indeed, deletion of Gata6 in the macrophage compartment resulted in a 60%–70% reduction in the number of peritoneal macrophages that were visible in the injury site at 6 hr post-injury (Figure 6A). Given a sufficient amount of time, macrophages from the Mac-*Gata6* KO mice were able to fill in the injured area but simply took longer to do so (Figure 6B). To assess whether Gata6 deficiency has an effect on macrophage recruitment, we transferred equal amount of labeled wild-type or Mac-*Gata6* KO macrophages separately to different recipients prior to injury, and comparable amounts of macrophages from both genotypes were noted at the injury sites (Figure 6C). Co-transfer of equal numbers of wild-type and Mac-*Gata6* KO macrophages that were labeled in different colors also

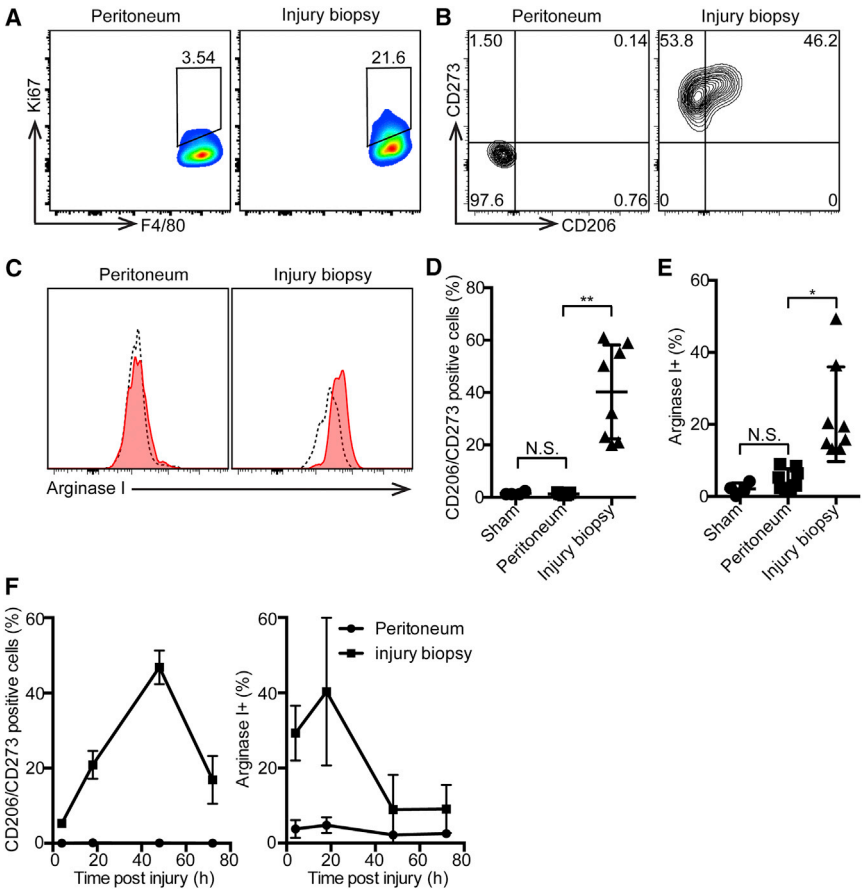


**Figure 4. Alternative Activation of Peritoneal Macrophages upon Accumulation at Injury**

(A) Representative flow cytometry analysis of Ki67 expression by macrophages isolated from peritoneal cavity or biopsies at 12 hr post-injury. Cells were pregated on size, viability, $CD45^+$, $CD11b^+$, and $F4/80^+$.

(B and C) Representative flow cytometry analysis of CD273/CD206 double-positive (B) or arginase-1-positive (C) populations of macrophages isolated from peritoneal cavity or injury biopsy at 24 hr post-injury. Cells were pregated on size, viability, $CD45^+$, $CD11b^+$, and $F4/80^+$. Red, arginase 1; dotted line, isotype control.

(D and E) Proportion of CD273/CD206 double-positive (D) or arginase-1-positive (E) populations of peritoneal macrophages isolated from peritoneal cavity of sham mice, or peritoneal cavity and injury biopsy from focal injury mice. Each symbol represents one mouse. Data were pooled from at least three independent experiments.

(F) Time course of CD206/CD273 (left) and arginase 1 (right) expression. n = 2.

Error bars represent SEM. *$p < 0.05$, **$p < 0.01$, N.S., not significant. See also Figure S4.

revealed similar amount of accumulation and distribution pattern at the injury site (Figure 6D). Clearly, the early recruitment of peritoneal macrophages seemed to be essential for tissue repair as the lesion size remained larger at 7 days in Mac-*Gata6* KO mice compared to wild-type mice (Figure 6E).

## Peritoneal Macrophages Invade into Liver in a Preclinical Liver Injury Model

To ensure that opening the peritoneal cavity during the injury did not have an untoward effect and also to address whether peritoneal macrophages are able to sense and respond to tissue damage within the liver, mice were orally administrated with carbon tetrachloride, a toxin that can cause pericentral cell injury and necrosis (Yu et al., 2002). A previous study has demonstrated a single dose of $CCl_4$ resulted in severe necroinflammatory injury that peaked at 24 hr and was resolved after 96 hr (de Meijer et al., 2010). Indeed, intravital imaging of injured liver with topically applied F4/80 antibody revealed large areas of avascular and necrotic regions, which were filled with F4/80-positive peritoneal macrophages (Figure 7A). The number of $F4/80^{hi}$ macrophages transiently increased at 24 hr and were decreased by 48 hr (Figure 7B). In contrast, liver from vehicle-treated control mice only had a very small number of $F4/80^{hi}$ cells (Figure S6A). To confirm that the infiltrating macrophages were derived from peritoneum, we transferred peritoneal macrophages from LyzM-eGFP mice and observed large numbers of LyzM-eGFP macrophages on the surface of liver lesions following $CCl_4$ administration (Figure 7C). In order to assess whether these macrophages can migrate across the mesothelium and penetrate into the intrahepatic area, cross-sections of the liver from LysM-eGFP peritoneal cells transferred mice were examined. We found $GFP^+$ macrophages crossing the mesothelium and able to penetrate many cell lengths into the injured tissue by 48 hr (Figure 7D). No $GFP^+$ macrophages were observed in the intrahepatic area in vehicle-treated control mice (Figure S6B). Immunostaining of cross-sections of injured liver using an antibody against mesothelial cell marker (podoplanin, PDPN) clearly labeled the surface of the liver (Figures 7E and S6C; Movies S6 and S7). Quantification of transferred $GFP^+$ cells within the first 500 μm in depth from the mesothelial layer showed many cells infiltrating at 24 hr with a few reaching to 500 μm depth. By 48 hr after $CCl_4$ treatment, there were many cells that had infiltrated at least 500 μm into the tissue (Figure 7F). We also harvested the whole liver and performed flow cytometry to determine the percentage of transferred $GFP^+$ macrophages in liver. Compared to vehicle-treated control mice, a substantially larger population of LyzM-$eGFP^+$ macrophages was found in the liver of $CCl_4$-treated mice (Figure 7G). To further address the role of peritoneal macrophages in $CCl_4$-induced hepatotoxicity, we compared the response of mice that have peritoneal macrophages depleted to control animals by measuring body weight after acute liver injury. Control mice that received $CCl_4$ lost about 5% body weight transiently but recovered fully within 72 hr. Mice that were depleted of peritoneal macrophages with clodronate showed a greater loss of body weight, and these mice continued losing weight and eventually were euthanized due to more than

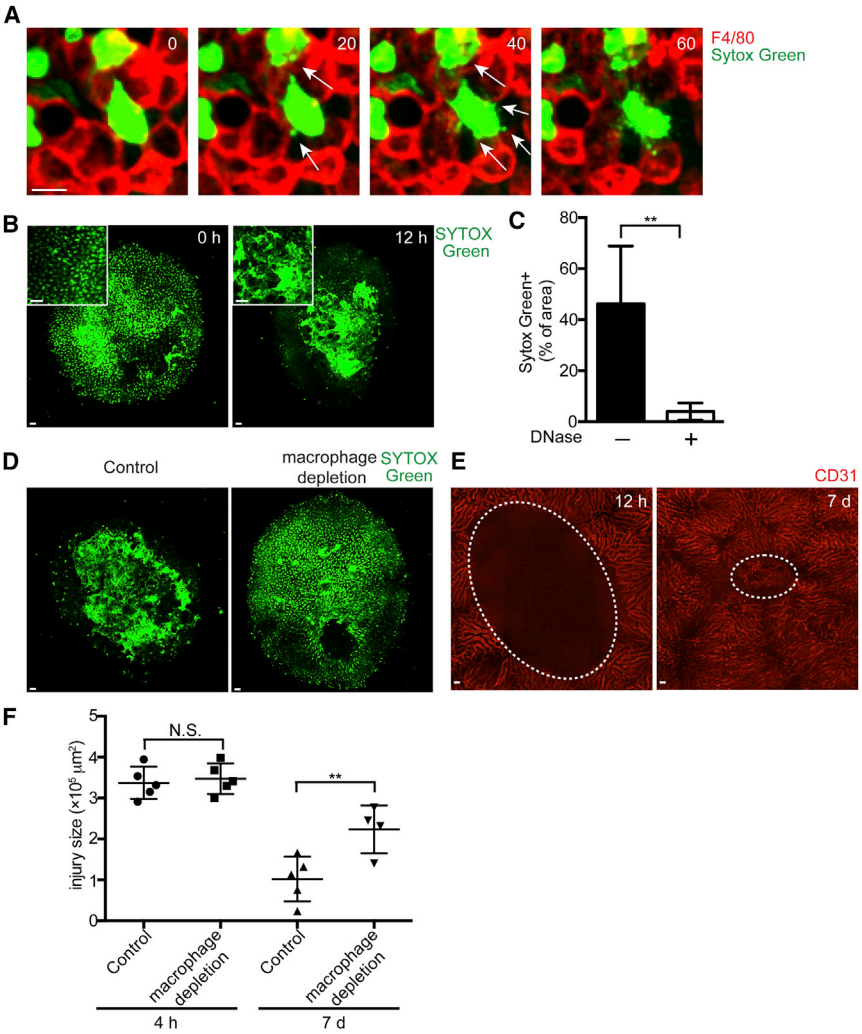


**Figure 5. Peritoneal Macrophages Ingest Necrotic DNA and Promote Tissue Repair and Revascularization**

(A) Time-lapse images showing macrophages (red) pulling off SYTOX Green particles (green) from nucleus body (still images from Movie S5). Elapsed time is shown in minutes. Scale bar, 10 μm.

(B) Representative images of necrotic cells (SYTOX Green, green) within injury at indicated time points. Scale bars, 15 and 40 μm (inset).

(C) Quantification of SYTOX Green$^+$ area within 12 hr of injury before and after topical application of DNase I. n = 3. Data are representative of two independent experiments.

(D) Representative images of necrotic cells within 12 hr of injury in PBS liposome (Control) or clodronate liposome (Macrophage depletion)-treated mice. Data are representative of five independent experiments. Scale bars, 15 μm.

(E) Representative images of injury lesion at indicated time points. Mice were intravenously injected with anti-CD31 (red) to visualize liver vasculature. White dashed line highlights injury border. Scale bars, 15 μm.

(F) Quantification of the size of injury lesion in PBS liposome (Control) or clodronate-liposome (macrophage depletion)-treated mice at 4 hr and 7 days post-injury. Each symbol represents one mouse. Data are representative of three independent experiments.

Error bars represent SEM. **p < 0.01. N.S., not significant. See also Figure S5 and Movie S5.

20% weight loss (Figure 7H). Administration of clodronate alone (without $CCl_4$) did not affect the body weight (data not shown). This result suggested that peritoneal macrophages possess protective effects on $CCl_4$-induced acute hepatotoxicity.

## DISCUSSION

The leukocyte recruitment pathway from blood to tissues is extremely well defined suggesting that selectins expressed on endothelium tether leukocytes to the vessel wall allowing them to roll with the flow of blood. The cells then adhere via integrins, due to activating molecules such as chemokines, which are immobilized to the vessel wall. The leukocytes then crawl through junctions between endothelial cells and ultimately emigrate out of the vasculature (Ley et al., 2007; Phillipson and Kubes, 2011). This mechanism is thought to be used by all immune cells, stem cells, and even some cancer cells. Inflammatory monocytes also use this recruitment cascade to get into tissues where they are thought to mature into macrophages. There are tissue resident macrophages in most if not all organs that have been proposed to perform many functions during inflammation including detecting disturbances and pathogens. They then release signals to (1) activate endothelium; (2) scavenge dead and dying cells including infiltrating neutrophils, and (3) ultimately help in remodeling or tissue repair (Davies et al., 2013a). However, resident macrophages are considered as stationary, and, to our knowledge, no study has ever shown these cells can move in liver, lung, and other organs. Indeed, using intravital microscopy, our previous studies also suggested that, in the liver, Kupffer cells reside in the vasculature and do not move either under basal conditions or in response to infections (Lee et al., 2010; Wong et al., 2013). As such, when significant tissue damage occurs, destroying the parenchyma and associated tissue macrophages, the prevailing view is that the system depends on monocyte recruitment from the vasculature to generate new macrophages for tissue repair (Das et al., 2015). Our data suggest that there is another, much more rapid way of recruiting mature macrophages to tissue injury from body cavities such as the peritoneum. Although pleural and pericardial cavities were not investigated in this study, these cavities also harbor resident macrophages (Nakatani et al., 1988; Shimotakahara et al., 2007), indicating macrophages in other cavities might have similar properties to peritoneal macrophages. This nonvascular, inter-organ, or cavity-organ recruitment occurs rapidly, via CD44 and the alarmin ATP and not by integrins and chemokines.

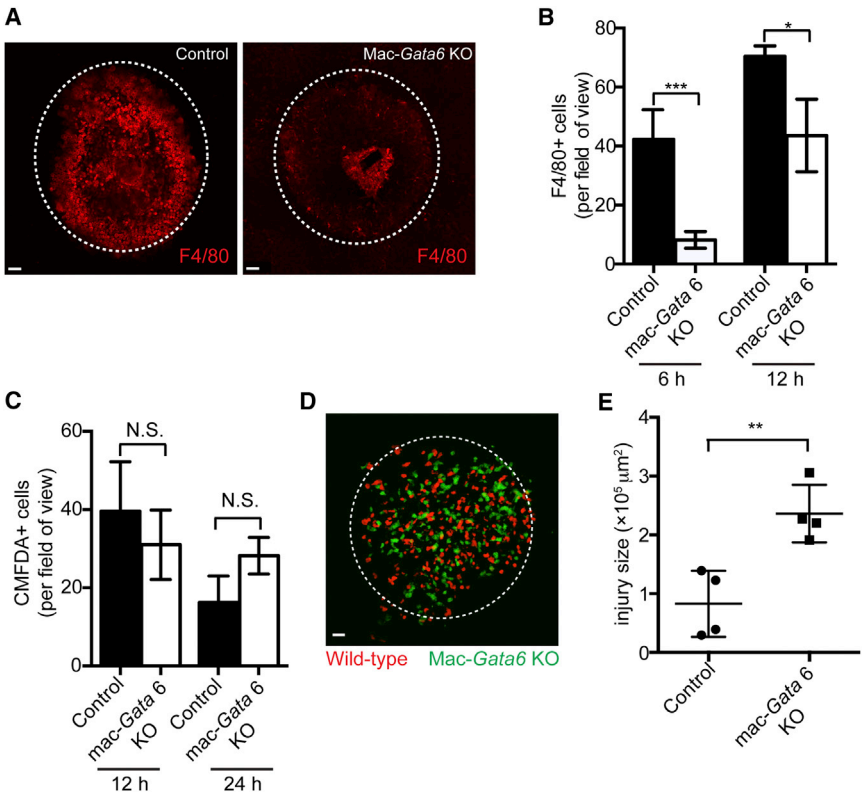


**Figure 6. Decreased Accumulation of Macrophages and Delayed Repair in GATA6-Deficient Mice**

(A) Representative images of F4/80$^{hi}$ macrophages within injury in wild-type (control) and Mac-*Gata6* KO mice at 6 hr post-injury. Scale bars, 15 μm.

(B) Quantification of F4/80$^{hi}$ macrophages at indicated time points in wild-type and Mac-*Gata6* KO mice. n = 3–4. Data were pooled from three independent experiments.

(C) Quantification of CMFDA-labeled wild-type and Mac-*Gata6* KO peritoneal cells inside the injury site at indicated time points. 3 × 10$^6$ labeled peritoneal cells from wild-type or Mac-*Gata6* KO were transferred into wild-type mice prior to injury. n = 2–3. Data were pooled from two independent experiments.

(D) Representative image of co-transferred wild-type (CMRA labeled, red) and Mac-*Gata6* KO (CMFDA labeled, green) peritoneal cells at 24 hr injury. 1 × 10$^6$ labeled peritoneal cells from each genotype were mixed at ratio of 1 and transferred into wild-type mice prior to injury. White dashed line highlights injury border. Scale bar, 15 μm. Data are representative of three independent experiments.

(E) Quantification of the size of injury lesion in wild-type and Mac-*Gata6* KO mice at 7 days post-injury. Each symbol represents one mouse. n = 4–5.

Data are representative of two independent experiments. Error bars represent SEM. *p < 0.05, **p < 0.01, ***p < 0.001, N.S., not significant.

A previous study has demonstrated ATP as a find-me signal (Elliott et al., 2009). However, extracellular ATP can be rapidly degraded, limiting the distance of a gradient set up by ATP. In fact, in vitro studies using resident peritoneal macrophages revealed that these cells do not migrate toward an ATP gradient in a classic chemotactic manner. Instead, ATP induced macrophage lamellipodial extensions and has been shown to act as a local "touch-me" signal by inducing macrophage spreading (Isfort et al., 2011). Unlike the tissue resident macrophage that are immobilized, macrophages in peritoneal cavity are floating within a small amount of peritoneal fluid, which is constantly circulating toward lymphatics in the undersurface of the diaphragm (Avraham-Chakim et al., 2013). This constantly flows the peritoneal macrophages over the abdominal organs making them much more ambulatory than tissue resident macrophages. When injury occurred, guidance molecules that were released or upregulated by cell death signals, such as ATP, induced arrest of this reservoir of mature macrophages. Although these macrophages bound to the surface of the wound, we also show that they also have the capacity to migrate across the mesothelial cells invading into the deeper tissue to perform their functions giving them a nomadic like phenotype.

Our working model raises an intriguing question, can other types of cells floating in the cavity also sense and respond to inflammatory signals derived from an inflamed organ that is in close proximity to the cavity and invade the afflicted tissue? Other than macrophages, B1 B cells are another dominant cell type in peritoneal and pleural cavity. Interestingly, a recent study of B1 B cells in pleural cavity suggested that these cells can relocate from pleural space to lung and produce protective immunoglobulin M (IgM) in response to microbial airway infection. However, the mechanism in this process was not studied (Weber et al., 2014). It is also worth noting that, although liver is the largest organ covered by the peritoneum, other visceral organs such as intestine and pancreas are also housed in the peritoneal cavity. Whether peritoneal macrophages can invade into these organs under pathological conditions needs to be studied in the future.

The mature GATA6$^+$ macrophages reside in the peritoneum in a less alternatively activated or default state, but once activated by injury-derived signals they can be rapidly induced to express numerous molecules associated with an alternative activated phenotype. Alternative activated macrophages have been suggested to exhibit tissue repair properties, showing attenuated production of pro-inflammatory cytokines and secretion of immunosuppressive cytokines (Martinez and Gordon, 2014). Consistent with a previous report, our results suggested tissue injury triggers rapid alternative activation of peritoneal macrophages (Loke et al., 2007). In fact, in our study significant alteration was noted within 4 hr of injury. The early activation of these macrophages may accelerate the end of classical inflammation and guarantee a rapid repair to maintain tissue integrity.

Because of the incredible ease with which these cells can be harvested from the peritoneum, many in vitro studies have attributed many functions to these cells including the ability to phagocytose apoptotic or necrotic cells (Brouckaert et al., 2004; Cocco

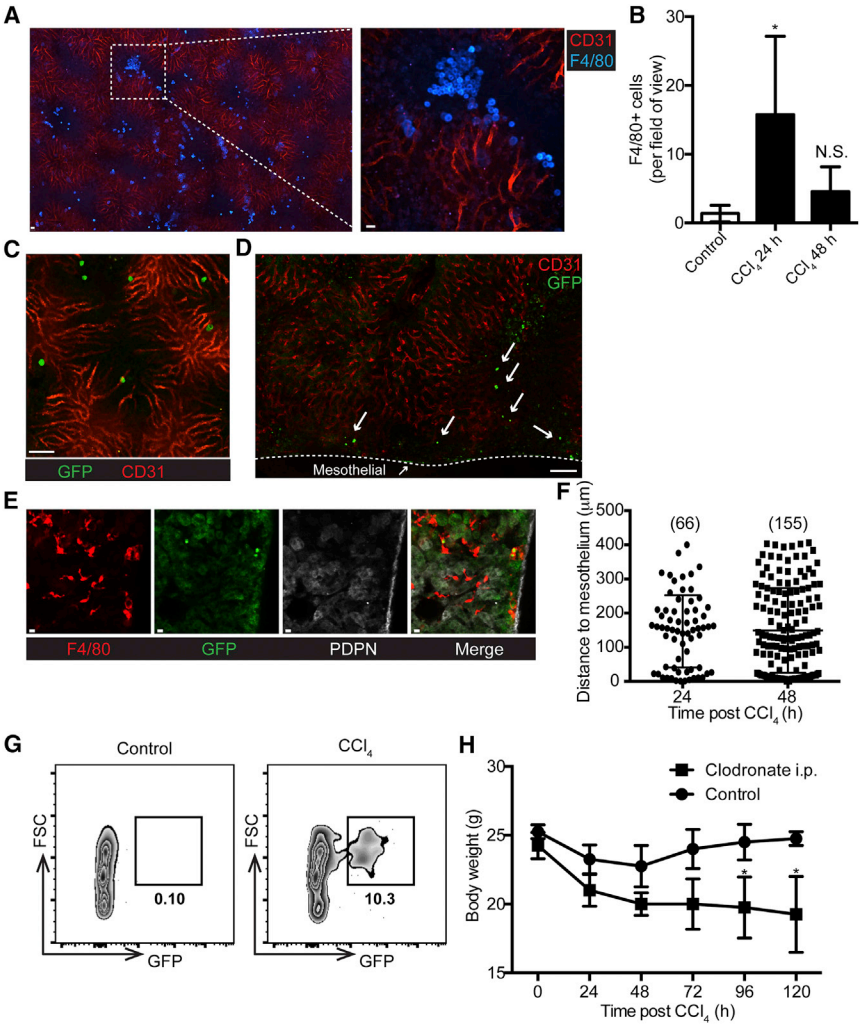


**Figure 7. Liver Invasion by Peritoneal Macrophages in Response to Carbon-Tetrachloride-Induced Hepatoxicity**

(A) Intravital image of liver lobe from $CCl_4$-treated mouse. F4/80 antibody (blue) was topically applied to the liver lobe and anti-CD31 (red) was given intravenously. Higher magnification of the indicated area (box) was shown in right. Scale bars, 15 μm.

(B) Number of F4/80$^{hi}$ cells in liver lobes as shown in (A) at indicated time points. Data were pooled from three independent experiments.

(C) Intravital image of liver lobe from $CCl_4$-treated mouse that received LysM-GFP peritoneal cells. Red, anti-CD31; green, LysM-eGFP. Scale bar, 50 μm.

(D) Cross-section of the liver lobe from mouse as indicated in (C). White dashed line highlights the border of mesothelium. Scale bar, 200 μm.

(E) Representative image of F4/80 (red) and podoplanin (PDPN, white) double immunostaining of liver sections at 24 hr post-$CCl_4$ treatment. Peritoneal cells from LysM-eGFP (arrows, green) mice were transferred intraperitoneally before treatment. Scale bars, 10 μm.

(F) Quantification of GFP$^+$ cells in liver sections that were double stained with F4/80 and PDPN. Numbers in parentheses indicate total cell numbers from 150 sections. Data were pooled from three independent experiments (n = 2–3).

(G) Flow cytometry analysis of isolated hepatic immune cell populations of vehicle- or $CCl_4$-treated mice that received 3 × 10$^6$ peritoneal cells from LysM-eGFP mice. Gated CD45$^+$/F4/80$^{high}$ population was further analyzed for percentage of GFP$^+$. Data are representative of three independent experiments.

(H) Weight loss in peritoneal-macrophage-depleted mice (clodronate intraperitoneally) and control mice (control) after acute $CCl_4$ treatment. Data are representative of three independent experiments.

Error bars represent SEM. *p < 0.05. N.S., not significant. See also Figure S6 and Movies S6 and S7.

and Ucker, 2001). By contrast, because these cells are free flowing in the peritoneum, they are impossible to image in vivo, and as such their function has not been visualized in detail. In this study, the cells were mobilized to the injured liver and could be observed to perform their functions in the in vivo environment. Our observation revealed that, instead of engulfing entire nuclei, macrophages ripped off small vesicles containing DNA from the necrotic nuclear body. This nibbling led to a dismantling of the nucleus releasing a large amount of free DNA covering the wound. Although our model had no infectious component, it is conceivable that the DNA and histones both with potent anti-microbial activity could now cover this barrier breach and protect the organ from invading bacteria. Indeed, neutrophils have been shown to release their own DNA and histones combined with numerous proteases and other anti-microbial molecules to help trap and eradicate bacteria. These DNA structures are called NETs. Herein, the release of DNA is very different, in that the macrophages were not releasing their own DNA, and there was no obvious amount of elastase and other proteases, a hallmark of NETs (Kolaczkowska and Kubes, 2013). However, despite a potential protective role in defending infection, subsequent clearance of this necrotic-cell-derived debris is needed to facilitate tissue repair. Further studies are needed to identify whether this extra-nuclear DNA might be taken up and ingested by macrophages or neutrophils or simply degraded by endogenous DNase.

The dismantling of the dead cells appeared to also be critical for revascularization and restoration of normal tissue. Indeed, if the peritoneal macrophages were depleted or the recruitment was delayed as shown in GATA6-deficient mice, the area that had been revascularized was much smaller. The liver has a tremendous capacity to heal, and one has to question whether this is in part due to the ability of the peritoneal macrophages to be recruited rapidly to the injured liver where they proliferated and helped by ingesting the dead tissue for rapid revascularization. In addition, in the carbon tetrachloride model, which is used to induce chronic injury and fibrosis, a single dose of this toxin induced hepatotoxicity and acute inflammation transiently,

followed by complete recovery. The macrophages helped in restitution, presumably through rapid clearance of the mass of cellular death and debris. In the absence of these cells, the liver remained injured and the mice were not able to repair. Clearly, the macrophages play a critical role in helping the liver overcome toxic insults. Although our approach was to examine the role for these peritoneal macrophages in sterile injury, one could imagine that these cells could also be recruited in hepatic cancers, liver infections, and in various chronic liver diseases. The role of peritoneal GATA6$^+$ macrophages should be evaluated in these models as an alternatively activated macrophage is thought to be potentially detrimental in the cancer environment where vascularization actually helps the tumor to grow (Noy and Pollard, 2014). Similarly, in certain chronic afflictions it could be possible that these macrophages may not present a beneficial repair phenotype but rather a more pro-inflammatory profile. It is worth noting that our work may have direct translation to the clinic when peritoneal dialysis as well as washing of peritoneal cavity during injury or infection is performed. Clearly, our work has opened a new area of study, namely, inter-organ invasion of a reservoir of cavity macrophages to altered or abnormal tissues where they may perform critical functions maintaining health and repair as is needed.

## EXPERIMENTAL PROCEDURES

### Mice

Mice were obtained from various sources and maintained in specific pathogen-free conditions. For details on mouse lines, see Supplemental Experimental Procedures.

### Flow Cytometry

The detailed procedures, antibodies used, and gate schemes are described in Supplemental Experimental Procedures.

### Peritoneal Cell Transfers

Peritoneal lavage was performed as described before using sterile PBS (Ghosn et al., 2010). Cells were washed with cold PBS twice and re-suspended in 100 μl PBS at different concentrations. Cells isolated from LysM-eGFP mice were directly transferred into naive mice. Both intraperitoneal and intravenous transfers were performed 1 hr prior to injury induction. Cells isolated from naive or Mac-*Gata6* KO mice were labeled with CellTracker Green CMFDA Dye (Thermo Fisher Scientific). The percentage of large peritoneal macrophages in labeled cells was determined by flow cytometry, and equal numbers of large peritoneal macrophages from different genotypes were transferred into naive mice by intraperitoneal administration. For co-transfer experiment, peritoneal cells from wild-type and Mac-*Gata6* KO mice were harvested and labeled with CellTracker Green CMFDA or Orange CMRA dyes (Thermo Fisher Scientific) separately. Viability after labeling was examined by flow cytometry. Wild-type and Mac-*Gata6* KO cells were mixed at 1:1 and intraperitoneally injected into non-fluorescent wild-type mice 1 hr prior to injury. The injury site was imaged at 24 hr.

### Sterile Inflammation Induced by Focal Necrotic Injury

Sterile inflammation induced by thermal injury in the liver was performed as described previously (Dal-Secco et al., 2015). In brief, mice were anesthetized with isoflurane, and a small incision was made just below the level of the diaphragm to expose the liver. A single focal injury was induced on the surface of the liver using the tip of a heated 30G needle mounted on an electrocautery device. The incision was sutured closed, and animals were allowed to recover for imaging of indicated time points after injury. For sham experiments, animals underwent the same surgical procedure but no thermal injury was induced.

### Imaging Studies

For details on immunofluorescence histology and intravital microscopy, see Supplemental Experimental Procedures.

### Statistical Analyses

Results are presented as mean ± SEM. Statistical analysis was performed in Prism 6 (GraphPad). Means between two groups were compared with t test. Means among three or more groups were compared with one-way or two-way ANOVA.

## SUPPLEMENTAL INFORMATION

Supplemental Information includes Supplemental Experimental Procedures, six figures, and seven movies and can be found with this article online at http://dx.doi.org/10.1016/j.cell.2016.03.009.

A video abstract is available at http://dx.doi.org/10.1016/j.cell.2016.03.009#mmc10.

## AUTHOR CONTRIBUTIONS

J.W. designed and performed experiments. J.W. and P.K. wrote the paper. P.K. conceived and supervised this study.

## ACKNOWLEDGMENTS

We thank all members of P.K.'s laboratory and the Live Cell Imaging Facility for training and assistance related to SD-IVM. We thank the University of Calgary Flow Cytometry Facility for assistance with the flow cytometry. We thank the Snyder Institute Bioinstrumentation Labs for assistance with the qRT-PCR. J.W. is supported by Banting Postdoctoral Fellowships Program. The P.K. lab is supported by Canadian Institute of Health Research and Alberta Innovates Health Solutions.

Received: November 23, 2015
Revised: February 1, 2016
Accepted: February 29, 2016
Published: April 7, 2016

## REFERENCES

Avraham-Chakim, L., Elad, D., Zaretsky, U., Kloog, Y., Jaffa, A., and Grisaru, D. (2013). Fluid-flow induced wall shear stress and epithelial ovarian cancer peritoneal spreading. PLoS ONE *8*, e60965.

Blériot, C., Dupuis, T., Jouvion, G., Eberl, G., Disson, O., and Lecuit, M. (2015). Liver-resident macrophage necroptosis orchestrates type 1 microbicidal inflammation and type-2-mediated tissue repair during bacterial infection. Immunity *42*, 145–158.

Brouckaert, G., Kalai, M., Krysko, D.V., Saelens, X., Vercammen, D., Ndlovu, M.N., Haegeman, G., D'Herde, K., and Vandenabeele, P. (2004). Phagocytosis of necrotic cells by macrophages is phosphatidylserine dependent and does not induce inflammatory cytokine production. Mol. Biol. Cell *15*, 1089–1100.

Cocco, R.E., and Ucker, D.S. (2001). Distinct modes of macrophage recognition for apoptotic and necrotic cells are not specified exclusively by phosphatidylserine exposure. Mol. Biol. Cell *12*, 919–930.

Dal-Secco, D., Wang, J., Zeng, Z., Kolaczkowska, E., Wong, C.H., Petri, B., Ransohoff, R.M., Charo, I.F., Jenne, C.N., and Kubes, P. (2015). A dynamic spectrum of monocytes arising from the in situ reprogramming of CCR2+ monocytes at a site of sterile injury. J. Exp. Med. *212*, 447–456.

Das, A., Sinha, M., Datta, S., Abas, M., Chaffee, S., Sen, C.K., and Roy, S. (2015). Monocyte and macrophage plasticity in tissue repair and regeneration. Am. J. Pathol. *185*, 2596–2606.

Davies, L.C., Jenkins, S.J., Allen, J.E., and Taylor, P.R. (2013a). Tissue-resident macrophages. Nat. Immunol. *14*, 986–995.

Davies, L.C., Rosas, M., Jenkins, S.J., Liao, C.T., Scurr, M.J., Brombacher, F., Fraser, D.J., Allen, J.E., Jones, S.A., and Taylor, P.R. (2013b). Distinct bone

marrow-derived and tissue-resident macrophage lineages proliferate at key stages during inflammation. Nat. Commun. *4*, 1886.

de Meijer, V.E., Sverdlov, D.Y., Popov, Y., Le, H.D., Meisel, J.A., Nosé, V., Schuppan, D., and Puder, M. (2010). Broad-spectrum matrix metalloproteinase inhibition curbs inflammation and liver injury but aggravates experimental liver fibrosis in mice. PLoS ONE *5*, e11256.

Elliott, M.R., Chekeni, F.B., Trampont, P.C., Lazarowski, E.R., Kadl, A., Walk, S.F., Park, D., Woodson, R.I., Ostankovich, M., Sharma, P., et al. (2009). Nucleotides released by apoptotic cells act as a find-me signal to promote phagocytic clearance. Nature *461*, 282–286.

Faust, N., Varas, F., Kelly, L.M., Heck, S., and Graf, T. (2000). Insertion of enhanced green fluorescent protein into the lysozyme gene creates mice with green fluorescent granulocytes and macrophages. Blood *96*, 719–726.

Gautier, E.L., Ivanov, S., Williams, J.W., Huang, S.C., Marcelin, G., Fairfax, K., Wang, P.L., Francis, J.S., Leone, P., Wilson, D.B., et al. (2014). Gata6 regulates aspartoacylase expression in resident peritoneal macrophages and controls their survival. J. Exp. Med. *211*, 1525–1531.

Ghosn, E.E., Cassado, A.A., Govoni, G.R., Fukuhara, T., Yang, Y., Monack, D.M., Bortoluci, K.R., Almeida, S.R., Herzenberg, L.A., and Herzenberg, L.A. (2010). Two physically, functionally, and developmentally distinct peritoneal macrophage subsets. Proc. Natl. Acad. Sci. USA *107*, 2568–2573.

Guidotti, L.G., Inverso, D., Sironi, L., Di Lucia, P., Fioravanti, J., Ganzer, L., Fiocchi, A., Vacca, M., Aiolfi, R., Sammicheli, S., et al. (2015). Immunosurveillance of the liver by intravascular effector CD8(+) T cells. Cell *161*, 486–500.

Herter, J., and Zarbock, A. (2013). Integrin regulation during leukocyte recruitment. J. Immunol. *190*, 4451–4457.

Huber, S., Hoffmann, R., Muskens, F., and Voehringer, D. (2010). Alternatively activated macrophages inhibit T-cell proliferation by Stat6-dependent expression of PD-L2. Blood *116*, 3311–3320.

Isfort, K., Ebert, F., Bornhorst, J., Sargin, S., Kardakaris, R., Pasparakis, M., Bähler, M., Schwerdtle, T., Schwab, A., and Hanley, P.J. (2011). Real-time imaging reveals that P2Y2 and P2Y12 receptor agonists are not chemoattractants and macrophage chemotaxis to complement C5a is phosphatidylinositol 3-kinase (PI3K)- and p38 mitogen-activated protein kinase (MAPK)-independent. J. Biol. Chem. *286*, 44776–44787.

Jenkins, S.J., Ruckerl, D., Cook, P.C., Jones, L.H., Finkelman, F.D., van Rooijen, N., MacDonald, A.S., and Allen, J.E. (2011). Local macrophage proliferation, rather than recruitment from the blood, is a signature of TH2 inflammation. Science *332*, 1284–1288.

Kim, N.D., and Luster, A.D. (2015). The role of tissue resident cells in neutrophil recruitment. Trends Immunol. *36*, 547–555.

Kolaczkowska, E., and Kubes, P. (2013). Neutrophil recruitment and function in health and inflammation. Nat. Rev. Immunol. *13*, 159–175.

Kono, H., and Rock, K.L. (2008). How dying cells alert the immune system to danger. Nat. Rev. Immunol. *8*, 279–289.

Lavine, K.J., Epelman, S., Uchida, K., Weber, K.J., Nichols, C.G., Schilling, J.D., Ornitz, D.M., Randolph, G.J., and Mann, D.L. (2014). Distinct macrophage lineages contribute to disparate patterns of cardiac recovery and remodeling in the neonatal and adult heart. Proc. Natl. Acad. Sci. USA *111*, 16029–16034.

Lee, W.Y., Moriarty, T.J., Wong, C.H., Zhou, H., Strieter, R.M., van Rooijen, N., Chaconas, G., and Kubes, P. (2010). An intravascular immune response to Borrelia burgdorferi involves Kupffer cells and iNKT cells. Nat. Immunol. *11*, 295–302.

Ley, K., Laudanna, C., Cybulsky, M.I., and Nourshargh, S. (2007). Getting to the site of inflammation: the leukocyte adhesion cascade updated. Nat. Rev. Immunol. *7*, 678–689.

Loke, P., Gallagher, I., Nair, M.G., Zang, X., Brombacher, F., Mohrs, M., Allison, J.P., and Allen, J.E. (2007). Alternative activation is an innate response to injury that requires CD4+ T cells to be sustained during chronic infection. J. Immunol. *179*, 3926–3936.

Martinez, F.O., and Gordon, S. (2014). The M1 and M2 paradigm of macrophage activation: time for reassessment. F1000Prime Rep. *6*, 13.

McDonald, B., McAvoy, E.F., Lam, F., Gill, V., de la Motte, C., Savani, R.C., and Kubes, P. (2008). Interaction of CD44 and hyaluronan is the dominant mechanism for neutrophil sequestration in inflamed liver sinusoids. J. Exp. Med. *205*, 915–927.

McDonald, B., Pittman, K., Menezes, G.B., Hirota, S.A., Slaba, I., Waterhouse, C.C., Beck, P.L., Muruve, D.A., and Kubes, P. (2010). Intravascular danger signals guide neutrophils to sites of sterile inflammation. Science *330*, 362–366.

Nakatani, T., Shinohara, H., Fukuo, Y., Morisawa, S., and Matsuda, T. (1988). Pericardium of rodents: pores connect the pericardial and pleural cavities. Anat. Rec. *220*, 132–137.

Noy, R., and Pollard, J.W. (2014). Tumor-associated macrophages: from mechanisms to therapy. Immunity *41*, 49–61.

Okabe, Y., and Medzhitov, R. (2014). Tissue-specific signals control reversible program of localization and functional polarization of macrophages. Cell *157*, 832–844.

Phillipson, M., and Kubes, P. (2011). The neutrophil in vascular inflammation. Nat. Med. *17*, 1381–1390.

Rayahin, J.E., Buhrman, J.S., Zhang, Y., Koh, T.J., and Gemeinhart, R.A. (2015). High and low molecular weight hyaluronic acid differentially influence macrophage activation. ACS Biomater. Sci. Eng. *1*, 481–493.

Rosas, M., Davies, L.C., Giles, P.J., Liao, C.T., Kharfan, B., Stone, T.C., O'Donnell, V.B., Fraser, D.J., Jones, S.A., and Taylor, P.R. (2014). The transcription factor Gata6 links tissue macrophage phenotype and proliferative renewal. Science *344*, 645–648.

Serhan, C.N., Brain, S.D., Buckley, C.D., Gilroy, D.W., Haslett, C., O'Neill, L.A., Perretti, M., Rossi, A.G., and Wallace, J.L. (2007). Resolution of inflammation: state of the art, definitions and terms. FASEB J. *21*, 325–332.

Shi, C., Velázquez, P., Hohl, T.M., Leiner, I., Dustin, M.L., and Pamer, E.G. (2010). Monocyte trafficking to hepatic sites of bacterial infection is chemokine independent and directed by focal intercellular adhesion molecule-1 expression. J. Immunol. *184*, 6266–6274.

Shimotakahara, A., Kuebler, J.F., Vieten, G., Metzelder, M.L., Petersen, C., and Ure, B.M. (2007). Pleural macrophages are the dominant cell population in the thoracic cavity with an inflammatory cytokine profile similar to peritoneal macrophages. Pediatr. Surg. Int. *23*, 447–451.

Uderhardt, S., Herrmann, M., Oskolkova, O.V., Aschermann, S., Bicker, W., Ipseiz, N., Sarter, K., Frey, B., Rothe, T., Voll, R., et al. (2012). 12/15-lipoxygenase orchestrates the clearance of apoptotic cells and maintains immunologic tolerance. Immunity *36*, 834–846.

Weber, G.F., Chousterman, B.G., Hilgendorf, I., Robbins, C.S., Theurl, I., Gerhardt, L.M., Iwamoto, Y., Quach, T.D., Ali, M., Chen, J.W., et al. (2014). Pleural innate response activator B cells protect against pneumonia via a GM-CSF-IgM axis. J. Exp. Med. *211*, 1243–1256.

Wong, C.H., Jenne, C.N., Petri, B., Chrobok, N.L., and Kubes, P. (2013). Nucleation of platelets with blood-borne pathogens on Kupffer cells precedes other innate immunity and contributes to bacterial clearance. Nat. Immunol. *14*, 785–792.

Yu, C., Wang, F., Jin, C., Wu, X., Chan, W.K., and McKeehan, W.L. (2002). Increased carbon tetrachloride-induced liver injury and fibrosis in FGFR4-deficient mice. Am. J. Pathol. *161*, 2003–2010.